

## Manuscript Details

<b>Manuscript number</b>	AQTOX_2018_388
<b>Title</b>	Effects of nanosilver on <i>Mytilus galloprovincialis</i> hemocytes and early embryo development
<b>Article type</b>	Research Paper

### Abstract

Silver nanoparticles (AgNP), one of the main nanomaterials for production and use, are expected to reach the aquatic environment, representing a potential threat to aquatic organisms. In this study, the effects of bare AgNPs (47nm) on the marine mussel *Mytilus galloprovincialis* were evaluated at the cellular and whole organism level utilizing both immune cells (hemocytes) and developing embryos. The effects were compared with those of ionic Ag<sup>+</sup> (AgNO<sub>3</sub>). In vitro short-term exposure (30 min) of hemocytes to AgNPs induced small lysosomal membrane destabilization (LMS EC<sub>50</sub> = 273.1 µg/ml) and did not affect other immune parameters (phagocytosis and ROS production). Responses were little affected by hemolymph serum (HS) as exposure medium in comparison to ASW. However, AgNPs significantly affected mitochondrial membrane potential and actin cytoskeleton at lower concentrations. AgNO<sub>3</sub> showed much higher toxicity, with an EC<sub>50</sub> = 1.23 µg/ml for LMS, decreased phagocytosis and induced mitochondrial and cytoskeletal damage at similar concentrations. Both AgNPs and AgNO<sub>3</sub> significantly affected *Mytilus* embryo development, with EC<sub>50</sub> = 23.7 and 1 µg/L, respectively. AgNPs caused malformations and developmental delay, but no mortality, whereas AgNO<sub>3</sub> mainly induced shell malformations followed by developmental arrest or death. Overall, the results indicate little toxicity of AgNPs compared with AgNO<sub>3</sub>; moreover, the mechanisms of action of AgNP appeared to be distinct from those of Ag<sup>+</sup>. The results indicate little contribution of released Ag<sup>+</sup> in our experimental conditions. These data provide a further insight into potential impact of AgNPs in marine invertebrates.

<b>Keywords</b>	Nanosilver; <i>Mytilus</i> ; hemocyte; immunity; mitochondria; cytoskeleton; embryos
<b>Taxonomy</b>	Aquatic Invertebrates, Early Embryonic Development, Nanoparticles, Bivalvia
<b>Corresponding Author</b>	Laura Canesi
<b>Corresponding Author's Institution</b>	Dept. of Earth, Environmental and Life Sciences, University of Genoa
<b>Order of Authors</b>	Manon Auguste, CATERINA CIACCI, teresa balbi, Andrea Brunelli, Valentina Caratto, Antonio Marcomini, Riccardo Cuppini, Laura Canesi
<b>Suggested reviewers</b>	Awadhesh Nandan Jha, Julian Blasco, M. Bebianno

## Submission Files Included in this PDF

### File Name [File Type]

CoverLetterAQ.doc [Cover Letter]

Highlights.docx [Highlights]

manuscript.docx [Manuscript File]

Fig1.tif [Figure]

Fig2.tif [Figure]

Fig3.tif [Figure]

Fig4.tif [Figure]

Fig5.tif [Figure]

Fig6.tif [Figure]

Fig7.tif [Figure]

To view all the submission files, including those not included in the PDF, click on the manuscript title on your EVISE Homepage, then click 'Download zip file'.

Dear Prof. Nikinmaa,

I send you the manuscript “Effects of nanosilver on *Mytilus galloprovincialis* hemocytes and early embryo development” to be considered for publication in Aquatic Toxicology.

The manuscript reports data of the in vitro and in vivo responses to AgNPs, one of the most widespread nanoparticle in use, in the model marine invertebrate *Mytilus galloprovincialis*. The effects and mechanism of action of bare AgNPs were investigated in short-term in vitro tests on mussel hemocytes using multiple end-points. Moreover, data are reposted on the effects on early embryo development. Parallel experiments were carried out using AgNO<sub>3</sub> as a soluble silver form.

Overall, the results indicate little toxicity of AgNPs compared with AgNO<sub>3</sub>; moreover, the mechanisms of action of AgNP appeared to be distinct from those of Ag<sup>+</sup>. These data provide a further insight into potential impact of AgNPs in marine invertebrates.

I thank you very much for your attention and look forward to hearing from you

Sincerely yours,

Laura Canesi

Dipartimento di Scienze della Terra, dell’Ambiente e della Vita- DISTAV, Università di Genova,  
Corso Europa 26, 16132, Italy

Tel: +39 010 3538241, Fax: +39 010 3538267.

[Laura.Canesi@unige.it](mailto:Laura.Canesi@unige.it)

## Highlights

- AgNPs do not affect immune parameters of *Mytilus* hemocytes in both ASW and HS
- AgNPs induced mitochondrial and cytoskeletal damage
- AgNPs decreased normal larval development and induced malformations in D-larvae
- AgNPs are much less toxic than Ag<sup>+</sup> in both mussel hemocytes and embryos
- The mechanisms of action of AgNPs appear to be distinct from those of Ag<sup>+</sup>

# **Effects of nanosilver on *Mytilus galloprovincialis* hemocytes and early embryo development**

M. Auguste<sup>1</sup>, C. Ciacci<sup>2</sup>, T. Balbi<sup>1</sup>, A. Brunelli<sup>3</sup>, V. Caratto<sup>4</sup>, A. Marcomini<sup>5</sup>, R. Cuppini<sup>2</sup>,  
L. Canesi<sup>1\*</sup>

<sup>1</sup>*Dept. of Earth, Environment and Life Sciences (DISTAV), University of Genoa, Genoa, Italy.*

<sup>2</sup>*Dept. of Biomolecular Sciences (DIBS), University of Urbino, Italy*

<sup>3</sup>*Dept. of Geosciences, University of Vienna, Austria*

<sup>4</sup>*Dept. of Chemistry and Industrial Chemistry (DICCI), University of Genoa, Genoa, Italy.*

<sup>5</sup>*Dept. of Environmental Sciences, Informatics and Statistics (DAIS), Ca' Foscari University, Venice, Italy*

\* Corresponding Author: [laura.canesi@unige.it](mailto:laura.canesi@unige.it)

## **Key words**

*Nanosilver, Mytilus, hemocyte, immunity, mitochondria, cytoskeleton, embryos*

## Abstract

Silver nanoparticles (AgNP), one of the main nanomaterials for production and use, are expected to reach the aquatic environment, representing a potential threat to aquatic organisms. In this study, the effects of bare AgNPs (47nm) on the marine mussel *Mytilus galloprovincialis* were evaluated at the cellular and whole organism level utilizing both immune cells (hemocytes) and developing embryos. The effects were compared with those of ionic Ag<sup>+</sup> (AgNO<sub>3</sub>). In vitro short-term exposure (30 min) of hemocytes to AgNPs induced small lysosomal membrane destabilization (LMS EC<sub>50</sub> = 273.1 µg/ml) and did not affect other immune parameters (phagocytosis and ROS production). Responses were little affected by hemolymph serum (HS) as exposure medium in comparison to ASW. However, AgNPs significantly affected mitochondrial membrane potential and actin cytoskeleton at lower concentrations. AgNO<sub>3</sub> showed much higher toxicity, with an EC<sub>50</sub> = 1.23 µg/ml for LMS, decreased phagocytosis and induced mitochondrial and cytoskeletal damage at similar concentrations.

Both AgNPs and AgNO<sub>3</sub> significantly affected *Mytilus* embryo development, with EC<sub>50</sub> = 23.7 and 1 µg/L, respectively. AgNPs caused malformations and developmental delay, but no mortality, whereas AgNO<sub>3</sub> mainly induced shell malformations followed by developmental arrest or death.

Overall, the results indicate little toxicity of AgNPs compared with AgNO<sub>3</sub>; moreover, the mechanisms of action of AgNP appeared to be distinct from those of Ag<sup>+</sup>. The results indicate little contribution of released Ag<sup>+</sup> in our experimental conditions. These data provide a further insight into potential impact of AgNPs in marine invertebrates.

## 1. Introduction

Silver nanoparticles (AgNPs) have a large number of applications for their chemico-physical characteristics and, above all, in virtue of their biocidal action. The widespread utilization of AgNPs in a large range of consumer products, including textiles, care products and food packaging, will inevitably lead to their release in the environment (reviewed in Pulit-Prociak and Banach, 2016; McGillicuddy et al., 2017). According to Gottschalk et al. (2009) Predicted Environmental Concentrations (PECs) of AgNP for surface water in Europe are expected to be in the low ng/L-range (0.76 ng/L), but it is expected to be released in larger quantities within the next decades (Fabrega et al., 2011; McGillicuddy et al., 2017). Once in the aquatic environment, AgNPs can undergo several transformation processes (agglomeration/aggregation, oxidation, dissolution, adsorption with soluble and particulate organic matter); in particular, release of Ag<sup>+</sup> ions may represent an additional source of silver in the environment (Levard et al., 2012; Sendra et al., 2017). With regards to ecotoxicity, it is widely acknowledged that the impact of AgNPs mainly depend on the Ag<sup>+</sup> released from the nanomaterial (Jemec et al., 2016). However, AgNPs may also exhibit a particle-specific toxicity, possibly mediated by physical interactions of the nanoparticulate form with biological systems (Li et al., 2014; Fabrega et al., 2011; Magesky and Pelletier 2018).

The impact of AgNPs has been widely investigated in marine invertebrates; these studies showed that *in vivo* exposure lead to silver accumulation, and different types of responses at molecular, cellular and tissue level (reviewed in Magesky and Pelletier 2018). The bivalve *Mytilus spp.* is considered a suitable model for studying the effects and mechanisms of action of different types of NPs (Canesi et al., 2012; Canesi and Procházová 2013; Canesi and Corsi, 2016). *In vivo* exposure to AgNPs have previously shown silver accumulation, induction of oxidative stress and damage to several cell components, including DNA (Zuykov et al., 2011; Gomes et al., 2013; McCarthy et al., 2013; Jimeno-Romero et al., 2017). These data provided valuable information at the whole organism level, also considering different potential pathway of exposure.

With regards to *in vitro* data, the application of a battery of functional tests on *Mytilus* immune cells, the hemocytes, has been proven as a powerful tool for the rapid *in vitro* screening of the immunomodulatory effects and identification of the mechanisms of action of different types of NPs (Canesi et al., 2012; Canesi and Procházková, 2013; Canesi and Corsi, 2016; Canesi et al., 2016). These studies also underlined the importance of exposure medium in determining particle behaviour and interactions with target cells in a physiological environment (Balbi et al., 2017a, Canesi et al., 2017). However, information on the impact of AgNPs in bivalves at the cellular level is scarce, with only one study available to date. Exposure of *M. galloprovincialis* hemocytes and gill cells to several types of maltose-coated AgNPs of different sizes revealed higher toxicity of smaller size NPs, damages to cell components and activation of cellular defences after 24 h (Katsumiti et al., 2015). These data underlined the importance to further investigate the *in vitro* effects of AgNPs in mussel cells, in order to better understand their mechanism of action and possible toxicity.

In marine invertebrates, NPs generally do not have lethal effects at environmental concentrations, but can induce changes in their life cycle, growth or anatomical deformities, that can lead to a diminished biological performance of wild populations (Canesi and Corsi 2016). The application of developmental assays, involving exposure during the most sensitive stages of the organisms to environmental contaminants, would greatly help in the fast screening of NP toxicity (Fabbri et al., 2014). Most data are available on the sea urchin model, where exposure to nanoparticulate and ionic silver induced distinct effects depending on the life stage (Šiller et al., 2013; Magesky and Pelletier 2018). Developmental effects were also reported for AgNPs in oysters (Ringwood et al., 2010). However, no information is available on the effects of AgNPs on *Mytilus* embryos.

In the present study, the effects of bare AgNPs were investigated at the cellular level in short term *in vitro* experiments of *M. galloprovincialis* hemocytes; the impact on mussel early embryo development was also evaluated. Parallel experiments were carried out using AgNO<sub>3</sub> in order to compare the effects of ionic silver. Hemocytes were exposed *in vitro* for 30 min to different

concentrations of AgNPs (0.1-1000 µg/ml) or AgNO<sub>3</sub> (0.1-10 µg/ml) and Lysosomal Membrane Stability (LMS) was first evaluated as a marker of cellular stress. Functional immune parameters were also evaluated (extracellular reactive oxygen species-ROS production, phagocytosis). Experiments with AgNPs were carried out in either artificial sea water (ASW) or hemolymph serum (HS) to evaluate the influence of exposure medium. Moreover, at selected concentrations of AgNPs and AgNO<sub>3</sub>, the effects on mitochondrial membrane potential and on actin cytoskeleton were evaluated by Confocal Laser Scanning Microscopy (CLSM).

The developmental effects of AgNPs were evaluated by the 48 h embryotoxicity test; fertilized eggs were exposed to AgNP (0.001-1000 µg/L) or AgNO<sub>3</sub> (0.1-25 µg/L). At the end of the assay, both percentage of normal D-larvae and the type of effect (malformations, delayed development, death) were evaluated.

## **2. Materials and methods**

### *2.1. Characterization of NPs*

AgNPs (47MN-03) were purchased from Advanced Materials Inframat. The sample is a silver, black and ultrafine nanopowder with no coating. Characterization of primary particles and AgNP suspensions were performed as previously described (Brunelli et al., 2013). The average size of particle distribution of primary particles was evaluated by HR-TEM (High Resolution Transmission Microscopy) using a JEOL (Tokyo, Japan) 3010 microscope operating at 300 kV. Specific surface area was evaluated using BET method by nitrogen adsorption on a Micromeritics (Norcross, GA, USA) ASAP 2000 instrument, with an adsorption temperature of -196 °C, and pre-treating under high vacuum at 300 °C for 2 h.

Particle suspensions were prepared using 20 mg of AgNPs powder in 20 ml of Artificial Marine Water (AMW, ASTM D1141-98; pH 7) and the suspension was sonicated for 15 min at 40 W,

pulsed 10% using a probe sonication in an ice bath. The desired dilutions were made in AMW or mussel hemolymph serum (HS). Both suspensions (10; 50; 100 mg/L for AMW and 10 mg/L for HS) were characterized: hydrodynamic size distribution and agglomeration were determined by Dynamic Light Scattering (DLS) with a Nicomp Submicron Particle Sizer Autodilute® Model 370 (Santa Barbara, CA, USA), using a 90° scattering angle (Brunelli, 2013).  $\zeta$ -potential values was measured using Electrophoretic light scattering.

For exposure experiments, AgNP was suspended in milliQ water at 1 mg/ml and homogenized using a probe sonication for 15 min in an ice bath. The next dilutions to obtain the desired exposure concentrations were made in either artificial seawater (ASW, pH 8) or hemolymph serum (HS), depending on the experiment. To obtain HS, the hemolymph was freshly extracted from mussels, filtered with gauze and centrifuged at 500 xg at 4°C for 10 min, and the supernatant was collected (Canesi et al., 2017). The different suspensions were in turn sonicated for 15 min prior to use. Stock solutions of silver nitrate (AgNO<sub>3</sub>) were prepared in milliQ water at 1 mg/ml and diluted in ASW to obtain the desired exposure concentrations.

## 2.2. *Mussels and hemocyte sample preparations*

Mussels (*M. galloprovincialis* Lam.), were purchased in 2017 from an aquaculture farm in the Ligurian Sea (La Spezia, Italy) out of the main spawning period (February-March) for hemocyte functional assays. Mussels were transferred to the laboratory and acclimatized in static tanks containing aerated artificial sea water-ASW (ASTM, 2004), pH 7.9-8.1, 36 ppt salinity (1 L/animal), at 16 ± 1 °C. Hemolymph was extracted from the adductor muscle of 4-5 animals, using a syringe with an 18 G1/2'' needle, filtered with gauze, and pooled. Hemocyte monolayers were prepared as previously described (Canesi et al., 2010).

### 2.3 Lysosomal membrane stability (LMS)

LMS was evaluated by the NRR (Neutral Red Retention time) assay as previously described (Ciacci et al., 2012; Canesi et al., 2010, 2015; Balbi et al., 2017b). Hemocyte monolayers on glass slides were incubated with 20  $\mu\text{l}$  of the AgNP suspension in filtered ASW or HS for 30 min to reach the desired final concentrations of 0.1-0.5-1-5-10-50-100-500-1000  $\mu\text{g/ml}$ . Parallel experiments were carried out with  $\text{AgNO}_3$  at the final concentrations of 0.1-0.2-0.5-1-1.5-2-10  $\mu\text{g/ml}$  in ASW. After incubation, the medium was removed and cells were incubated with a neutral red (NR) solution (final concentration 40  $\mu\text{g/ml}$  from a stock solution of NR 40 mg/ml in DMSO); after 15 min excess dye was washed out and 20  $\mu\text{l}$  of ASW was added. Every 15 min, slides were examined under an optical microscope and the percentage of cells showing loss of the dye from lysosomes in each field was evaluated. For each time point 10 fields were randomly observed, each containing 8–10 cells. The end point of the assay was defined as the time at which 50% of the cells showed sign of lysosomal leaking (the cytosol becoming red and the cells rounded). All incubations were carried out at 16 °C.

### 2.4. Confocal Laser Scanning Microscopy (CLSM)

Hemocytes were exposed to AgNPs (5, 10, 50  $\mu\text{g/ml}$  in ASW) or  $\text{AgNO}_3$  (0.2 and 1  $\mu\text{g/ml}$ ) for 30 min. Cells were fixed with paraformaldehyde at 4% for 10 min, washed two times for 2 min with TBS (0.05 M Tris-HCl buffer, pH 7.8) and permeabilized with 0.05%NP-40 (Nonidet-40) for 10 min.

Mitochondrial membrane potential (MMP,  $\Delta\psi\text{m}$ ) was evaluated by the fluorescent dye Tetramethylrhodamine ethyl ester perchlorate (TMRE) as previously described (Ciacci et al., 2012; Canesi et al., 2008, 2015). TMRE is a quantitative marker for the maintenance of the mitochondrial membrane potential and it is accumulated within the mitochondrial matrix in accordance to the Nernst equation. TMRE exclusively stains the mitochondria and is not retained in cells upon

collapse of the  $\Delta\psi_m$ . Hemocytes were incubated with 40 nM TMRE for 10 min and observed by confocal microscopy.

Actin cytoskeleton structure was evaluated in hemocytes loaded with ActinGreen<sup>TM</sup>488 ReadyProbes<sup>®</sup> Reagent for 30 min to reveal F-actin.

Fluorescence of TMRE (excitation 568 nm, emission 590-630 nm), and ActinGreen<sup>TM</sup>488 (excitation 495 nm, emission 518 nm) was detected using a Leica TCS SP5 confocal setup mounted on a Leica DMI 6000 CS inverted microscope (Leica Microsystems, Heidelberg, Germany) using a 63x 1.4 oil objective (HCX PL APO 63.0-1.40 OIL UV). Images were analysed by the Leica Application Suite Advanced Fluorescence (LASAF) and ImageJ Software (Wayne Rasband, Bethesda, MA).

### *2.5 Mussels and gamete collection*

Mussels sampled at the main spawning season (Feb-March) were transferred to the laboratory and acclimatized in static tanks containing aerated artificial sea water (ASTM, 2004), pH 7.9-8.1, 36 ppt salinity (1 L/animal), at  $16 \pm 1^\circ\text{C}$ . Mussels were utilized within 2 days for gamete collection as previously described (Fabbri et al., 2014). When mussels beginning to spontaneously spawn were observed, each individual was immediately placed in a 250 mL beaker containing 200 mL of aerated ASW until complete gamete emission. After spawning, mussels were removed from beakers and sperms and eggs were sieved through 50  $\mu\text{m}$  and 100  $\mu\text{m}$  meshes, respectively, to remove impurities. Egg quality (shape, size) and sperm motility were checked using an inverted microscope. Eggs were fertilized with an egg:sperm ratio 1:10 in polystyrene 96-microwell plates (Costar, Corning Incorporate, NY, USA). After 30 min fertilization success (n. fertilized eggs / n. total eggs  $\times$  100) was verified by microscopical observation (>85%).

### *2.6 Embryotoxicity test*

The 48-h embryotoxicity assay (ASTM, 2004) was carried out in 96-microwell plates according to Fabbri et al. (2014). Aliquots of 20  $\mu\text{L}$  of 10x suspensions of AgNPs or of  $\text{AgNO}_3$  solutions, suitably diluted in filter sterilized ASW, were added to fertilized eggs in each microwell to reach the nominal final concentrations (0-1000  $\mu\text{g/L}$  for AgNPs and 0-25  $\mu\text{g/L}$  for  $\text{AgNO}_3$ ) in a 200  $\mu\text{L}$  volume. Microplates were gently stirred for 1 min, and then incubated at  $18 \pm 1^\circ\text{C}$  for 48 h, with a 16 h:8 h light:dark photoperiod. At the end of the incubation time, samples were fixed with buffered formalin (4%). A larva was considered normal when the shell was D-shaped (straight hinge) and the mantle did not protrude out of the shell, and malformed if had not reached the stage typical for 48 h (trocophora or earlier stages) or when some developmental defects were observed (concave, malformed or damaged shell, protruding mantle). The recorded endpoint was the percentage of normal D-larvae in each well respect to the total, including malformed larvae and pre-D stages. The acceptability of test results was based on controls for a percentage of normal D-shell stage larvae  $>75\%$  (ASTM, 2004). Three experiments were made using 6 wells replicates per conditions. All larvae in each well were examined by optical microscopy using an inverted Olympus IX53 microscope (Olympus, Milano, Italy) at 400x, equipped with a CCD UC30 camera and a digital image acquisition software (cellSens Entry).

### 2.7. Statistics

Data, representing the mean  $\pm$  SD of 4 experiments, were analysed by ANOVA followed by Tukey's post-test ( $p \leq 0.05$ ). For embryotoxicity test, data, representing the mean  $\pm$  SD of 3 independent experiments, carried out in 6 replicates in 96-microwell plates. The  $\text{EC}_{50}$  was defined as the concentration causing 50% reduction in the number of D-veligers at a 95% confidence interval (CI). All statistic calculations were performed by the PRISM 7 GraphPad software.

## 3. Results

### 3.1 AgNP characterization

In Fig.1 are reported the data on physico-chemical characterization of AgNP. Primary particle characterization showed that AgNPs are formed by irregular elongated polyhedrons and spherical particles with rounded and smooth edges (Fig. 1A, TEM images). The Z-average particle size obtained was 61 nm, with value ranging between 41 and 81 nm (64% of particles comprised between 35 and 65 nm) (Fig.1A distribution graph by frequency), very similar as the declared value (i.e. 40-90 nm). The sample presented little inorganic element impurities of Fe ( $24 \pm 2 \mu\text{g/g}$ ) and Ca ( $0.5 \pm 0.1 \mu\text{g/g}$ ) and a specific surface area obtained by BET method of  $3.8 \pm 0.1 \text{ m}^2/\text{g}$ . Characterization of particle suspensions in two exposure media (Fig.1B), ASW (10, 50, 100 mg/ml) and hemolymph serum (HS) (10 mg/L) was performed. DLS analysis of AgNPs in ASW showed the formation of two populations of agglomerates whose size increased with concentration (10, 50, 100 mg/L). Smaller agglomerates ( $138 \pm 20$ ;  $130 \pm 22$ ;  $340 \pm 55$  nm for each concentration respectively), represented less than a third of the whole population, whereas the majority was represented by larger agglomerates ( $671 \pm 122$ ;  $590 \pm 99$ ;  $1600 \pm 340$  nm). A similar behaviour was observed for AgNP suspensions in HS (10 mg/L), with two populations of AgNPs,  $89 \pm 18$  nm and  $473 \pm 57$  nm, that were slightly smaller than those observed in ASW at the same concentration. Values of  $\zeta$ -potential were similar at different concentrations in ASW (between -1.1 mv and -1.8 mV) and the same in both media at the same concentration (10 mg/L) ( $-1.5 \pm 3.7$  mV).

### 3.2. Hemocyte functional responses

The short term *in vitro* effects of different concentrations of AgNPs on *M. galloprovincialis* hemocytes were compared in ASW and HS, since different exposure media have been shown to influence the toxicity of certain types of NPs (Canesi et al., 2015, 2016, 2017). Hemocytes were exposed for 30 min to different concentrations (up to 1000  $\mu\text{g/ml}$ ) of AgNPs in ASW or HS and Lysosomal membrane stability (LMS) was first evaluated as a marker of cellular stress; the results are reported in Fig. 2. As shown in Fig. 2A, exposure of hemocytes to AgNPs in ASW induced a

significant and dose dependent decrease in LMS from 5 to 100  $\mu\text{g/ml}$  (-17% to -38%, respectively;  $P \leq 0.05$ ). A further decrease in LMS was observed at higher concentrations, together with cell detachment and death due to the presence of large agglomerates (not shown). A similar trend was observed for AgNP suspensions in HS. However, a slightly higher effect was observed with HS with respect to ASW only at 100  $\mu\text{g/mL}$  (-50% in HS vs -38% in ASW;  $P \leq 0.05$ ).

Exposure to  $\text{AgNO}_3$  induced a sharp dose-dependent decrease in LMS, that was significant from 0.5  $\mu\text{g/ml}$  (-18% with respect to control;  $P \leq 0.05$ ). A complete destabilization was observed at 2  $\mu\text{g/ml}$  (Fig. 2B).

The distinct effects between AgNPs in ASW and  $\text{AgNO}_3$  were compared by evaluating their  $\text{EC}_{50}$  values. For AgNP suspensions in ASW the  $\text{EC}_{50}$  was 273.1  $\mu\text{g/ml}$  (95% CI: 184.9-442.5  $\mu\text{g/ml}$ ). For  $\text{AgNO}_3$  an  $\text{EC}_{50}$  of 1.23  $\mu\text{g/ml}$  (95% CI: 0.83-1.84  $\mu\text{g/ml}$ ) was obtained.

Due to the small difference in LMS observed in different exposure media, other parameters related to the immune function were measured using AgNP suspensions in ASW. AgNPs did not affect the phagocytic ability at any concentration tested from 5 to 100  $\mu\text{g/ml}$  (Fig. 3A). In contrast,  $\text{AgNO}_3$  caused a dose dependent decrease in phagocytic ability from 0.2  $\mu\text{g/ml}$  ( $P \leq 0.05$ ) (Fig. 3B). Neither AgNPs or  $\text{AgNO}_3$ , induced extracellular ROS release (data not shown).

### *3.3 Effect on mitochondrial parameters and cytoskeleton*

The effects of hemocyte incubation with AgNPs (30 min) on mitochondria were evaluated by cell staining with TMRE (Tetramethylrhodamine, ethyl ester perchlorate) an indicator of mitochondrial membrane potential  $\Delta\psi\text{m}$ , and representative CLSM images are reported in Fig. 4. At lower concentrations (5  $\mu\text{g/ml}$ ) AgNPs did not affect TMRE fluorescence (not shown), whereas at 50  $\mu\text{g/ml}$  a clear decrease was observed with respect to controls (Fig. 4A and B). AgNP agglomerates of different sizes ( $\mu\text{m}$ ) were observed in the extracellular medium, with smaller agglomerates apparently taken up by the cells (Fig. 4B, right panel). Lower concentrations of

AgNO<sub>3</sub> (0.2 µg/ml) were ineffective (not shown). However, at higher concentrations (1 µg/ml) AgNO<sub>3</sub> decreased TMRE fluorescence and induced cell rounding (Fig. 4C).

The effects of AgNPs on cytoskeletal structures of mussel hemocytes were evaluated by ActinGreen™488 staining, that reveals the architecture of cytosolic microfilaments, and representative CLSM images are shown in Fig. 5. Control hemocytes showed extended lamellipodia and cytoplasmic prolongations with the presence of thin microspikes, indicating strong adhesion to the substrate (Fig. 5A). In hemocytes exposed to lower concentrations of AgNPs (5 and 10 µg/ml), a general decrease in the cytoplasmic signal was observed; however, cells retained their adherent shape, with evident microspikes (Fig. 5B and 5C). In contrast, after exposure to higher concentrations (50 µg/ml), cells adopted a round shape with smaller cell extensions, and the actin signal was often concentrated at the edge of the cells, close to the plasma membrane (Fig. 5D-F). In hemocytes exposed to AgNO<sub>3</sub>, a decrease in the cytoplasmic actin signal with respect to controls was observed at concentrations as low as 0.2 µg/ml, although cell morphology was unaffected (Fig. 5G). At higher concentrations (1 µg/ml), AgNO<sub>3</sub> induced cell rounding and blebbing, indicating extensive cell damage and loss of adhesion (Fig. 5H).

### 3.4 Embryotoxicity test

Fertilized eggs were exposed to different concentrations (from 0.001 to 1000 µg/L) of AgNPs in 96-microwell plates, and the percentage of normal D-larvae was evaluated after 48 h as previously described (Fabbri et al., 2014; Balbi et al., 2017c). In controls, the percentage of normal D-larvae at 48 h was 82 ± 5%. The results, reported in Fig. 6, show that AgNPs induced a dose-dependent decrease in normal larval development, with an EC<sub>50</sub> = 23.7 µg/L (20.8 – 26.9 µg/L). The effect was significant from 10 µg/L (-30%; P ≤ 0.01) and was dramatic (-75%) from concentrations ≥ 60 µg/L (Fig. 6A). As shown in Fig. 6B, at concentrations below EC<sub>50</sub>, a dose-dependent increase in malformed D-veligers was observed. A rise in the percentage of immature D-larvae and trocophorae was detected at higher concentrations. From concentrations of 80 - 100

$\mu\text{g/L}$ , AgNPs completely inhibited the formation of the D-shaped veliger, with about 75% of the larvae withheld at the trocophora stage. Representative images of control and AgNPs-exposed larvae are reported in Fig. 6 (C1-C3). Fig.6 C1 shows a normal D-veliger after 48h post fertilization with a characteristic D-shape. At 20  $\mu\text{g/L}$  malformed larvae were observed (42% of total embryos); the characteristic D-shape was altered showing shell indentations and protruding mantle (Fig.6 C2). At higher concentrations (100  $\mu\text{g/L}$ ), larval development was delayed, with a majority of embryos at the trocophorae stage (C3).

The effects of  $\text{AgNO}_3$  on embryo development were also evaluated, and the results are reported in Fig. 7.  $\text{AgNO}_3$  induced a sharp dose-dependent decrease in normal embryo development, with an  $\text{EC}_{50}$  value of 1  $\mu\text{g/L}$  (0.5 – 1.9  $\mu\text{g/L}$ ) (Fig. 7A), with most embryos showing strong shell malformations (Fig. 7B). From 5  $\mu\text{g/L}$ , no normal D-veligers were observed;  $\text{AgNO}_3$  prevented development of fertilized eggs or resulted in dead trocophorae (not shown).

#### 4. Discussion

Marine invertebrates can represent a significant target for the impact of nanosilver (Magesky and Pelletier, 2018), one of the most widespread NP type (Pulit-Prociak and Banach, 2016). In this work, data are presented on the effects of bare AgNPs (47 nm) in the marine bivalve *M. galloprovincialis* evaluated at the cellular and whole organism level using two model systems i.e. short term *in vitro* exposure of hemocytes and the 48 h embryotoxicity assay. The effects were compared with those of  $\text{AgNO}_3$ .

##### 4.1 Effects on hemocytes

High ionic strength media promote the formation of large AgNP agglomerates of several hundreds of nm, often represented by two main populations (Li et al., 2012; Yin et al., 2015). Accordingly, the results here presented show that in ASW AgNPs form large agglomerates of increasing size at

increasing concentrations, with constant formation of two populations, the majority represented by larger agglomerates of hundred nms (Fig. 1). The results are comparable with other data on behaviour of different types of AgNPs in ASW (Sendra et al., 2017, Schiavo et al., 2017). No differences in  $\zeta$ -potential were observed in ASW and HS, with values close to the point of zero charge ( $-1.5 \pm 3.7$  mV). Moreover, at 10 mg/L, agglomeration was lower in HS than in ASW: such an effect was previously observed with amino modified nanopolystyrene PS-NH<sub>2</sub> and nCeO<sub>2</sub> (Canesi et al., 2016; Canesi et al., 2017). These data indicate that in the experimental conditions utilized for most *in vitro* tests ( $\leq 100$   $\mu$ g/ml) the major part of AgNPs will be present in the form of agglomerates. Indeed, larger AgNP agglomerates of micrometric size were observed in the extracellular medium and smaller agglomerates were apparently internalized by hemocytes. These observations are important for considering and understanding the response of hemocytes towards AgNPs. The results of functional parameters indicate little toxicity of AgNPs in mussel hemocytes. Although a dose-dependent decrease in LMS was observed, from 5  $\mu$ g/ml, EC<sub>50</sub> values were extremely high (273.1  $\mu$ g/ml). Accordingly, no changes were observed in phagocytosis and extracellular ROS production at concentrations up to 100  $\mu$ g/ml in both ASW and HS. The lack of disturbance of immune-related parameters suggests that in our experimental conditions AgNP agglomerates have little interactions at the level of the cell membrane. The results are in line with those previously obtained in cells from *M. galloprovincialis* exposed to maltose-coated AgNPs for longer periods of time (Katsumiti et al., 2015).

In this work, the effects of AgNPs were also investigated in the presence of different exposure media (in ASW and HS). The importance of the exposure media has been emphasized when testing NPs in different cell models, including mussel hemocytes (Ren et al., 2016; Canesi et al., 2017). Data on identification of NP protein coronas for PS-NH<sub>2</sub> and nCeO<sub>2</sub> suggested that the net surface charge retained by the particles in high ionic strength media, such as mussel hemolymph, might be an important factor in the formation of a stable protein corona, that can increase or decrease particle interactions with hemocytes (Canesi et al. 2017). The results here obtained seem to reinforce this

hypothesis: AgNPs displayed a quasi-neutral surface charge in both ASW and HS, and the presence of HS had little effect on lysosomal membrane stability, indicating that interactions with protein serum components seem to little affect the response of hemocyte to AgNPs.

AgNPs are known to be highly corroded in presence of salts and oxygen and can release silver ions ( $\text{Ag}^+$ ) in high ionic strength media like ASW (Liu and Hurt, 2010; Levard et al., 2012). In order to investigate the complementary role of ions released from NPs, parallel experiments were performed using silver nitrate ( $\text{AgNO}_3$ ) to evaluate the effects of  $\text{Ag}^+$  in its soluble form.  $\text{AgNO}_3$  induced a dramatic decrease in LMS, with an  $\text{EC}_{50}$  as low as 1  $\mu\text{g}/\text{ml}$ . Moreover, in the same concentration range,  $\text{AgNO}_3$  induced a dose-dependent inhibition of the phagocytic activity. These data indicate a much stronger and distinct effect of  $\text{Ag}^+$  in comparison with AgNPs in mussel hemocytes.

The short term *in vitro* effects of NPs on mussel hemocytes have been thoroughly evaluated by measuring different endpoints related to lysosomal function, phagocytosis, oxyradical production, apoptosis, with LMS being considered the most sensitive endpoint (Canesi et al., 2012; Canesi and Procházková, 2013, Canesi and Corsi et al., 2016). However, certain NP types (nanosized carbon black-NCB, PS- $\text{NH}_2$  and n-ZnO) have been shown to affect also mitochondrial parameters and pre-apoptotic processes (Canesi et al., 2008, 2015; Ciacci et al., 2012).

The results here presented show that AgNPs induced a rapid decrease in mitochondrial membrane potential at 50  $\mu\text{g}/\text{ml}$ , a concentration much lower than the  $\text{EC}_{50}$  for LMS. Alteration of  $\Delta\psi_m$  by AgNPs was recorded for several mammalian and human cells (Asharani et al., 2009; Singh and Romarao 2012; Yang et al., 2012). AgNPs can strongly interact with membrane thiol groups (-SH) and stay immobilized near the membrane, including the mitochondrial membrane, where they can interfere with protons present in the intermembrane space thus affecting the electron flow and possibly enhancing the formation of ROS (Lapestra-Fernandez et al., 2012; Yang et al., 2012; Zhang et al., 2014). Also exposure to  $\text{AgNO}_3$  reduced mitochondrial membrane potential, although at much lower concentrations; a clear decrease in TMRE fluorescence accompanied by cell rounding was observed at 1  $\mu\text{g}/\text{ml}$ , thus paralleling the effects on lysosomal membranes.

AgNPs also affected hemocyte cytoskeletal structures, with a decrease in immunofluorescence of filamentous actin from 5  $\mu\text{g/ml}$ ; at higher concentrations (50  $\mu\text{g/ml}$ ), morphological changes were also observed, with cells adopting a round shape with smaller extensions; moreover, a concentration of the actin signal in the peripheral part of the cells was observed. The effects of AgNPs on cytoskeletal structures are in line with previous data obtained both in mussel hemocytes (Katsumiti et al., 2015) and in human cells (Zhao et al., 2017), although at longer exposure time (hours). Cytoskeletal alterations induced by AgNPs may be ascribed to AgNP dissolution;  $\text{Ag}^+$  ions may act directly, by binding to actin filaments causing depolymerisation, or indirectly, through alterations of  $\text{Ca}^{2+}$  homeostasis, mitochondrial damage and ROS production (Asharani et al., 2009; Singh and Romarao 2012; Gomes et al., 2013; Zhao et al., 2017). However, AgNPs show a strong binding capacity for both actin and tubulin *in vitro*, altering secondary structures of the proteins and in particular perturbing the structural integrity of the alpha helices of actin (Wen et al., 2013). The results here obtained indicate that the effects of AgNPs on actin cytoskeleton in mussel hemocytes are extremely rapid, occurring at 30 min of exposure and at concentrations that did not cause strong lysosomal damage or impairment of immune parameters. In contrast,  $\text{AgNO}_3$  severely affected actin cytoskeleton, and induced cell rounding at much lower concentrations (0.2-1  $\mu\text{g/ml}$ ), in parallel with decreased LMS and phagocytic activity, indicating extensive cellular damage.

Overall, the results indicate that in our experimental conditions mitochondria and cytoskeletal structures represent the main targets of AgNPs; however, these data do not indicate a toxicity scenario mediated by  $\text{Ag}^+$  release. Indeed, on the basis of extensive literature data, in our experimental conditions AgNP should not release  $\text{Ag}^+$  in sufficient quantities to contribute to the overall effects observed in short time exposure experiments (30 min) (Sendra et al., 2017; Schiavo et al., 2017; Liu and Hurt, 2010; Levard et al., 2012). This hypothesis is reinforced by the large gap in effective concentrations and type of effect between the nanoparticulate and soluble  $\text{Ag}^+$  forms.

#### 4.2. Effects on embryo development

For environmental regulatory purposes, data on early life stages of aquatic species are important to establish the sensitivity of a species to different contaminants. The 48 h bivalve embryotoxicity test represents a standardized and reproducible protocol that allows the sensitive evaluation of the early developmental effects of a number of both legacy and emerging pollutants (ASTM, 2004, ASTM, 2012; Fabbri et al., 2014).

The present results demonstrate that AgNPs significantly affect *M. galloprovincialis* early development. A sharp dose-dependent decrease in the percentage of normal embryos was recorded in a narrow concentration range (10-100 µg/L), with an EC<sub>50</sub> of 23.7 µg/L. At lower concentrations, the characteristic D-shape of embryos was altered, showing shell indentations and protruding mantle. Moreover, from 40 µg/L, an increase in immature embryos was observed, indicating progressive developmental arrest. Similarly, embryos of the oyster *Crassostrea virginica* exposed to AgNPs of smaller size (15 nm) showed a decrease in normal development; the effects were observed at low µg/L concentrations, although particle behaviour and type of developmental effect were not evaluated (Ringwood et al., 2010). Higher concentrations of citrate stabilized AgNPs (5-35 nm) have been shown to induce developmental toxicity in the sea urchin *Paracentrotus lividus* at 48 hpf. (Šiller et al., 2013). All together, these data suggest that different types of AgNPs may have a significant impact on embryo development in marine invertebrates.

Moreover, our data show that in *M. galloprovincialis* embryos AgNPs had stronger detrimental effects compared to other types of NPs. Exposure to stabilized zero-valent nanoiron (nZVI) resulted in a decrease in normal D-shaped mussel embryos, with significant effects from concentrations ≤ 100 µg/L (Kadar et al., 2011). In contrast, n-TiO<sub>2</sub> did not affect embryo development at concentrations lower than 4 mg/L (Libralato et al., 2012; Balbi et al., 2014). Similarly, nCeO<sub>2</sub> was ineffective up to 1 mg/L (Canesi, unpublished results).

When the embryotoxicity of ionic  $\text{Ag}^+$  was evaluated using  $\text{AgNO}_3$ , obtained  $\text{EC}_{50}$  values ( $1 \mu\text{g/L}$ ) were more than twenty times lower than that of AgNPs and similar to that induced by  $\text{Cu}^{2+}$ , the reference metal used as positive control in the embryotoxicity assay (Fabbri et al., 2014).

In comparison with short term *in vitro* tests with hemocytes, the effects of AgNPs over the time course of the embryotoxicity assay (48 h) may be the result of metal dissolution in ASW, as shown for different types of AgNPs, depending on particle size, agglomeration, pH and coating, with smaller and coated AgNPs releasing more  $\text{Ag}^+$  (Katsumiti et al., 2015; Schiavo et al., 2017; Sendra et al., 2017). Although in the present study the release of  $\text{Ag}^+$  was not evaluated, Schiavo et al. (2017) showed that for the same AgNP type (uncoated 47nm AgNPs) released  $\text{Ag}^+$  in ASW was about 0.6- 1.5- 3% at 0, 24 and 48 h, respectively. If this were the case, at the  $\text{EC}_{50}$  for AgNPs of  $23.7 \mu\text{g/L}$  embryos would be exposed to a maximum of  $0.7 \mu\text{g/L}$   $\text{Ag}^+$  at the end of the assay (48 h) and to much lower concentrations at shorter times of exposure ( $0.14$ ,  $0.35 \mu\text{g/L}$ , respectively, for fertilized eggs and trocophorae at 0 and 24 h pf). The lower impact of AgNP on embryos compared to  $\text{AgNO}_3$  could be related to the limited amount of bioavailable nanomaterial due to high agglomeration state of AgNPs in ASW. Moreover, the type of effects of AgNPs on embryo development were distinct from those of ionic  $\text{Ag}^+$ . AgNPs caused malformations and developmental delay, but no mortality, in a wide concentration range, whereas  $\text{AgNO}_3$  mainly induced shell malformations followed by developmental arrest or death.

The data reported in the present study represent a first attempt to compare the possible effects and mechanism of action of AgNPs and soluble  $\text{Ag}^+$  in mussels at the cellular and organism level. In both experimental settings, AgNPs was effective at much higher concentrations than those of  $\text{AgNO}_3$ , indicating little toxicity; moreover, the mechanisms of action of AgNP appeared to be distinct from those of  $\text{Ag}^+$  in both hemocytes and embryos. Overall, the results provide a further insight into the effects and mechanisms of action of AgNPs in marine invertebrates.

## Funding

This project has received funding from the European Union's Horizon 2020 research and innovation programme under the Marie Skłodowska-Curie grant agreement PANDORA N° 671881.

## References

- Asharani, P.V., Low Kah Mun, G., Hande, M.P., Valiyaveetil, S., 2009. Cytotoxicity and Genotoxicity of Silver Nanoparticles in Human Cells. *ACS Nano* 3, 279–290. <https://doi.org/10.1021/nm800596w>
- ASTM, 2004. Standard Guide for Conducting Static Acute Toxicity Tests Starting with Embryos of Four Species of Saltwater Bivalve Molluscs. <http://dx.doi.org/10.1520/E0724-98>.
- ASTM, 2012. Standard Guide for Conducting Static Acute Toxicity Tests Starting with Embryos of Four Species of Saltwater Bivalve Molluscs. <http://dx.doi.org/10.1520/E0724-98R12>
- ASTM D1141-98, 2013. Standard Practice for the Preparation of Substitute Ocean Water, <https://doi.org/10.1520/D1141-98R13>
- Balbi, T., Caratto, V., Fabbri, R., Camisassi, G., Villa, S., Ferretti, M., Canesi, L., 2017a. Photocatalytic Fe-doped n-TiO<sub>2</sub>: From synthesis to utilization of *in vitro* cell models for screening human and environmental nanosafety. *Resource-Efficient Technologies* 3, 158–165. <https://doi.org/10.1016/j.reffit.2017.03.009>
- Balbi, T., Fabbri, R., Montagna, M., Camisassi, G., Canesi, L., 2017b. Seasonal variability of different biomarkers in mussels (*Mytilus galloprovincialis*) farmed at different sites of the Gulf of La Spezia, Ligurian sea, Italy. *Mar Pollut Bull* 116, 348–356. <https://doi.org/10.1016/j.marpolbul.2017.01.035>
- Balbi, T., Camisassi, G., Montagna, M., Fabbri, R., Franzellitti, S., Carbone, C., Dawson, K., Canesi, L., 2017c. Impact of cationic polystyrene nanoparticles (PS-NH<sub>2</sub>) on early embryo development of *Mytilus galloprovincialis*: Effects on shell formation. *Chemosphere* 186, 1–9. <https://doi.org/10.1016/j.chemosphere.2017.07.120>
- Balbi, T., Smerilli, A., Fabbri, R., Ciacci, C., Montagna, M., Grasselli, E., Brunelli, A., Pojana, G., Marcomini, A., Gallo, G., Canesi, L., 2014. Co-exposure to n-TiO<sub>2</sub> and Cd<sup>2+</sup> results in interactive effects on biomarker responses but not in increased toxicity in the marine bivalve *M. galloprovincialis*. *Sci Total Environ* 493, 355–364. <https://doi.org/10.1016/j.scitotenv.2014.05.146>
- Brunelli, A., Pojana, G., Callegaro, S., Marcomini, A., 2013. Agglomeration and sedimentation of titanium dioxide nanoparticles (n-TiO<sub>2</sub>) in synthetic and real waters. *J Nanopart Res* 15. <https://doi.org/10.1007/s11051-013-1684-4>
- Brunelli Andrea, 2013 «Advanced physico-chemical characterization of engineered nanomaterials in nanotoxicology», PhD Thesis, University Ca' Foscari Venice, Italy; 172 p.
- Canesi, L., Ciacci, C., Betti, M., Fabbri, R., Canonico, B., Fantinati, A., Marcomini, A., Pojana, G., 2008. Immunotoxicity of carbon black nanoparticles to blue mussel hemocytes. *Environ Int* 34, 1114–1119. <https://doi.org/10.1016/j.envint.2008.04.002>
- Canesi, L., Ciacci, C., Vallotto, D., Gallo, G., Marcomini, A., Pojana, G., 2010. *In vitro* effects of suspensions of selected nanoparticles (C60 fullerene, TiO<sub>2</sub>, SiO<sub>2</sub>) on *Mytilus* hemocytes. *Aquat Toxicol* 96, 151–158. <https://doi.org/10.1016/j.aquatox.2009.10.017>
- Canesi, L., Ciacci, C., Fabbri, R., Marcomini, A., Pojana, G., Gallo, G., 2012. Bivalve molluscs as a unique target group for nanoparticle toxicity. *Mar Environ Res* 76, 16–21. <https://doi.org/10.1016/j.marenvres.2011.06.005>

- Canesi L. and Procházová P., 2013. The invertebrate immune system as a model for investigating the environmental impact of nanoparticles, in: Boraschi D, Duschl A, (Eds.), Nanoparticles and the immune system. Oxford Academic Press, pp. 91-112.
- Canesi, L., Ciacci, C., Bergami, E., Monopoli, M.P., Dawson, K.A., Papa, S., Canonico, B., Corsi, I., 2015. Evidence for immunomodulation and apoptotic processes induced by cationic polystyrene nanoparticles in the hemocytes of the marine bivalve *Mytilus*. *Mar Environ Res* 111, 34–40. <https://doi.org/10.1016/j.marenvres.2015.06.008>
- Canesi, L., Ciacci, C., Balbi, T., 2016. Invertebrate Models for Investigating the Impact of Nanomaterials on Innate Immunity: The Example of the Marine Mussel *Mytilus spp.* *Current Bionanotechnol* 2, 77–83. <https://doi.org/10.2174/2213529402666160601102529>
- Canesi, L. and Corsi, I., 2016. Effects of nanomaterials on marine invertebrates. *Sci Total Environ* 565, 933–940. <https://doi.org/10.1016/j.scitotenv.2016.01.085>
- Canesi, L., Balbi, T., Fabbri, R., Salis, A., Damonte, G., Volland, M., Blasco, J., 2017. Biomolecular coronas in invertebrate species: Implications in the environmental impact of nanoparticles. *NanoImpact* 8, 89–98. <https://doi.org/10.1016/j.impact.2017.08.001>
- Ciacci, C., Canonico, B., Bilaničová, D., Fabbri, R., Cortese, K., Gallo, G., Marcomini, A., Pojana, G., Canesi, L., 2012. Immunomodulation by Different Types of N-Oxides in the Hemocytes of the Marine Bivalve *Mytilus galloprovincialis*. *PLoS ONE* 7, e36937. <https://doi.org/10.1371/journal.pone.0036937>
- Fabbri, R., Montagna, M., Balbi, T., Raffo, E., Palumbo, F., Canesi, L., 2014. Adaptation of the bivalve embryotoxicity assay for the high throughput screening of emerging contaminants in *Mytilus galloprovincialis*. *Marine Environmental Research* 99, 1–8. <https://doi.org/10.1016/j.marenvres.2014.05.007>
- Fabrega, J., Luoma, S.N., Tyler, C.R., Galloway, T.S., Lead, J.R., 2011. Silver nanoparticles: Behaviour and effects in the aquatic environment. *Environ Int* 37, 517–531. <https://doi.org/10.1016/j.envint.2010.10.012>
- Gomes, T., Pereira, C.G., Cardoso, C., Bebianno, M.J., 2013. Differential protein expression in mussels *Mytilus galloprovincialis* exposed to nano and ionic Ag. *Aquat Toxicol* 136–137, 79–90. <https://doi.org/10.1016/j.aquatox.2013.03.021>
- Gottschalk, F., Sonderer, T., Scholz, R.W., Nowack, B., 2009. Modeled environmental concentrations of engineered nanomaterials (TiO<sub>2</sub>, ZnO, Ag, CNT, fullerenes) for different regions. *Environ Sci Technol* 43, 9216–9222.
- Jemec, A., Kahru, A., Potthoff, A., Drobne, D., Heinlaan, M., Böhme, S., Geppert, M., Novak, S., Schirmer, K., Rekulapally, R., Singh, S., Aruoja, V., Sihtmäe, M., Juganson, K., Käkinen, A., Kühnel, D., 2016. An interlaboratory comparison of nanosilver characterisation and hazard identification: Harmonising techniques for high quality data. *Environ Int* 87, 20–32. <https://doi.org/10.1016/j.envint.2015.10.014>
- Jimeno-Romero, A., Bilbao, E., Izagirre, U., Cajaraville, M.P., Marigómez, I., Soto, M., 2017. Digestive cell lysosomes as main targets for Ag accumulation and toxicity in marine mussels, *Mytilus galloprovincialis*, exposed to maltose-stabilised Ag nanoparticles of different sizes. *Nanotoxicology* 11, 168–183. <https://doi.org/10.1080/17435390.2017.1279358>
- Kadar, E., Tarran, G.A., Jha, A.N., Al-Subiai, S.N., 2011. Stabilization of Engineered Zero-Valent Nanoiron with Na-Acrylic Copolymer Enhances Spermotoxicity. *Environ Sci Technol* 45, 3245–3251. <https://doi.org/10.1021/es1029848>
- Katsumiti, A., Gilliland, D., Arostegui, I., Cajaraville, M.P., 2015. Mechanisms of Toxicity of Ag Nanoparticles in Comparison to Bulk and Ionic Ag on Mussel Hemocytes and Gill Cells. *PLOS ONE* 10, e0129039. <https://doi.org/10.1371/journal.pone.0129039>
- Lapresta-Fernández, A., Fernández, A., Blasco, J., 2012. Nanoecotoxicity effects of engineered silver and gold nanoparticles in aquatic organisms. *TrAC* 32, 40–59. <https://doi.org/10.1016/j.trac.2011.09.007>

- Levard, C., Hotze, E.M., Lowry, G.V., Brown, G.E., 2012. Environmental Transformations of Silver Nanoparticles: Impact on Stability and Toxicity. *Environ Sci Technol* 46, 6900–6914. <https://doi.org/10.1021/es2037405>
- Li, X., Lenhart, J.J., Walker, H.W., 2012. Aggregation Kinetics and Dissolution of Coated Silver Nanoparticles. *Langmuir* 28, 1095–1104. <https://doi.org/10.1021/la202328n>
- Li, L., Wu, H., Peijnenburg, W.J., van Gestel, C.A., 2014. Both released silver ions and particulate Ag contribute to the toxicity of AgNPs to earthworm *Eisenia fetida*, *Nanotoxicology*, 9:6, 792-801, <https://doi.org/10.3109/17435390.2014.976851>
- Libralato, G., Minetto, D., Totaro, S., Mičetić, I., Pigozzo, A., Sabbioni, E., Marcomini, A., Volpi Ghirardini, A., 2013. Embryotoxicity of TiO<sub>2</sub> nanoparticles to *Mytilus galloprovincialis* (Lmk). *Mar Environ Res* 92, 71–78. <https://doi.org/10.1016/j.marenvres.2013.08.015>
- Liu, J. and Hurt, R.H., 2010. Ion Release Kinetics and Particle Persistence in Aqueous Nano-Silver Colloids. *Environ Sci Technol* 44, 2169–2175. <https://doi.org/10.1021/es9035557>
- McCarthy, M.P., Carroll, D.L., Ringwood, A.H., 2013. Tissue specific responses of oysters, *Crassostrea virginica*, to silver nanoparticles. *Aquat Toxicol* 138–139, 123–128. <https://doi.org/10.1016/j.aquatox.2013.04.015>
- McGillicuddy, E., Murray, I., Kavanagh, S., Morrison, L., Fogarty, A., Cormican, M., Dockery, P., Prendergast, M., Rowan, N., Morris, D., 2017. Silver nanoparticles in the environment: Sources, detection and ecotoxicology. *Sci Total Environ* 575, 231–246. <https://doi.org/10.1016/j.scitotenv.2016.10.041>
- Magesky, A., Pelletier, E., 2018. Cytotoxicity and Physiological Effects of Silver Nanoparticles on Marine Invertebrates, in: Saquib, Q., Faisal, M., Al-Khedhairi, A.A., Alatar, A.A., (Eds.), *Cellular and Molecular Toxicology of Nanoparticles*. Springer International Publishing, pp.285-309. <https://doi.org/10.1007/978-3-319-72041-8>
- Pulit-Prociak, J., Banach, M., 2016. Silver nanoparticles – a material of the future...? *Open Chem* 14. <https://doi.org/10.1515/chem-2016-0005>
- Ren, C., Hu, X., Zhou, Q., 2016. Influence of environmental factors on nanotoxicity and knowledge gaps thereof. *NanoImpact* 2, 82–92. <https://doi.org/10.1016/j.impact.2016.07.002>
- Ringwood, A.H., McCarthy, M., Bates, T.C., Carroll, D.L., 2010. The effects of silver nanoparticles on oyster embryos. *Mar Environ Res* 69, S49–S51. <https://doi.org/10.1016/j.marenvres.2009.10.011>
- Schiavo, S., Duroudier, N., Bilbao, E., Mikolaczyk, M., Schäfer, J., Cajaraville, M.P., Manzo, S., 2017. Effects of PVP/PEI coated and uncoated silver NPs and PVP/PEI coating agent on three species of marine microalgae. *Sci Total Environ* 577, 45–53. <https://doi.org/10.1016/j.scitotenv.2016.10.051>
- Sendra, M., Yeste, M.P., Gatica, J.M., Moreno-Garrido, I., Blasco, J., 2017. Direct and indirect effects of silver nanoparticles on freshwater and marine microalgae (*Chlamydomonas reinhardtii* and *Phaeodactylum tricornutum*). *Chemosphere* 179, 279–289. <https://doi.org/10.1016/j.chemosphere.2017.03.123>
- Šiller, L., Lemloh, M.-L., Piticharoenphun, S., Mendis, B.G., Horrocks, B.R., Brümmer, F., Medaković, D., 2013. Silver nanoparticle toxicity in sea urchin *Paracentrotus lividus*. *Environ Pollut* 178, 498–502. <https://doi.org/10.1016/j.envpol.2013.03.010>
- Singh, R.P., Ramarao, P., 2012. Cellular uptake, intracellular trafficking and cytotoxicity of silver nanoparticles. *Toxicol Lett* 213, 249–259. <https://doi.org/10.1016/j.toxlet.2012.07.009>
- Wen, Y., Geitner, N.K., Chen, R., Ding, F., Chen, P., Andorfer, R.E., Govindan, P.N., Ke, P.C., 2013. Binding of cytoskeletal proteins with silver nanoparticles. *RSC Advances* 3, 22002. <https://doi.org/10.1039/c3ra43281e>
- Yang, E.-J., Kim, S., Kim, J.S., Choi, I.-H., 2012. Inflammasome formation and IL-1 $\beta$  release by human blood monocytes in response to silver nanoparticles. *Biomaterials* 33, 6858–6867. <https://doi.org/10.1016/j.biomaterials.2012.06.016>

- Yin, Y., Yang, X., Zhou, X., Wang, W., Yu, S., Liu, J., Jiang, G., 2015. Water chemistry controlled aggregation and photo-transformation of silver nanoparticles in environmental waters. *J Environ Sci* 34, 116–125. <https://doi.org/10.1016/j.jes.2015.04.005>
- Zhang, T., Wang, L., Chen, Q., Chen, C., 2014. Cytotoxic Potential of Silver Nanoparticles. *Yonsei Med J* 55, 283. <https://doi.org/10.3349/ymj.2014.55.2.283>
- Zhao, X., Toyooka, T., Ibuki, Y., 2017. Silver nanoparticle-induced phosphorylation of histone H3 at serine 10 is due to dynamic changes in actin filaments and the activation of Aurora kinases. *Toxicol Lett* 276, 39–47. <https://doi.org/10.1016/j.toxlet.2017.05.009>
- Zuykov, M., Pelletier, E., Demers, S., 2011. Colloidal complexed silver and silver nanoparticles in extrapallial fluid of *Mytilus edulis*. *Mar Environ Res* 71, 17–21. <https://doi.org/10.1016/j.marenvres.2010.09.004>

### Figures captions

**Figure 1** - Physico-chemical characterization of bare 47 nm AgNPs (Inframat® Advanced Materials).

A) Primary particle characterization. Top left: Z-average (nm), inorganic element impurities evaluated by ICP-OES and specific surface area by BET method. Bottom left: Particle size distribution graph by frequency. Right: TEM images.

B) Characterization of AgNP suspensions in artificial seawater (ASW) and *Mytilus* hemolymph serum (HS), using DLS analysis showing Z-average (nm) and  $\zeta$ -potential (mV). Data are reported as mean  $\pm$  SD.

**Figure 2** - Effects of AgNPs and AgNO<sub>3</sub> on Lysosomal membrane stability (LMS) of *Mytilus* hemocytes. Hemocytes were exposed for 30 min to different concentrations of AgNPs and LMS was evaluated by the NRR time assay (A). AgNP suspensions in either ASW or hemolymph serum (HS) were utilized. Parallel experiments were carried out using different concentrations of AgNO<sub>3</sub> diluted in ASW (B). Data, representing the mean  $\pm$  SD of four experiments in triplicate, were analysed by ANOVA followed by Tukey's post hoc test ( $p < 0.05$ ); \* = all treatments vs controls; # = HS vs ASW.

**Figure 3** - Effects of AgNPs and AgNO<sub>3</sub> in ASW on phagocytic activity of *Mytilus* hemocytes, A) AgNPs; B) AgNO<sub>3</sub>. Data, representing the mean ± SD of three experiments in triplicate, were analysed by ANOVA followed by Tukey's post hoc test. Significant differences with respect to controls ( $p < 0.05$ ) are reported (\*).

**Figure 4** - Confocal fluorescence microscopy: effects of exposure of *Mytilus* hemocytes to AgNPs and AgNO<sub>3</sub> (30 min) on mitochondrial membrane potential ( $\Delta\psi_m$ ) evaluated by TMRE fluorescence. Control and treated hemocytes were loaded with TMRE (and representative images are reported (568 excitation/ 590-630 emission) (Left panels). A) Control hemocytes; B) hemocytes exposed to AgNPs (50 µg/ml); C) hemocytes exposed to AgNO<sub>3</sub>: 0.2 µg/ml. In right panels light microscopy images are also reported: B) shows the presence of large AgNP agglomerates in the extracellular medium (arrowheads) and of smaller agglomerates apparently taken up by the cells (arrows). In C), cell rounding induced by AgNO<sub>3</sub> can be observed. Scale bar: 25 µm.

**Figure 5** - Confocal fluorescence microscopy: effects of exposure of *Mytilus* hemocytes to AgNPs and AgNO<sub>3</sub> (30 min) on actin cytoskeleton. Control and treated hemocytes were loaded with ActinGreen™488 and representative images are reported (495 excitation/518 emission): A) Control hemocytes; B-F) hemocytes exposed to AgNPs: B) 5 µg/ml, C) 10 µg/ml and D-F) 50 µg/ml; G-H) Hemocytes exposed to AgNO<sub>3</sub> : G) 0.2 µg/ml and H) 1 µg/ml. Scale bar: 25 µm.

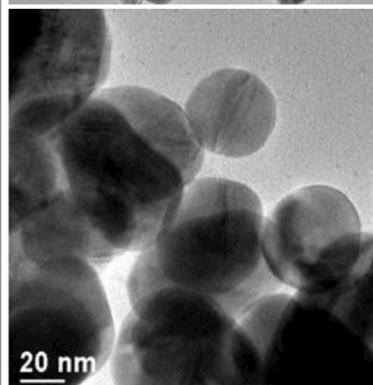
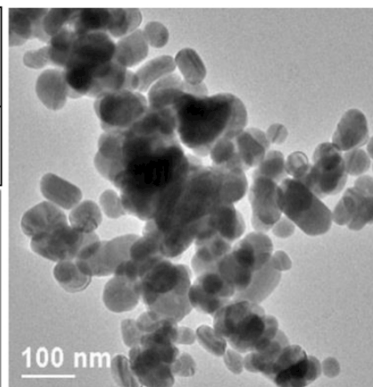
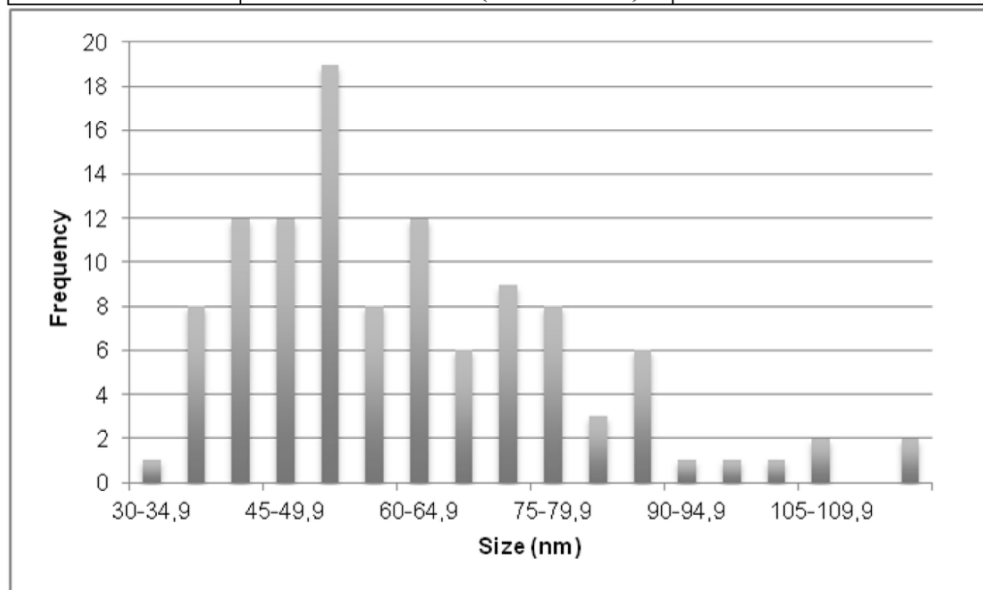
**Figure 6** - Effects of AgNPs on *M. galloprovincialis* larval development evaluated in the 48 h embryotoxicity assay. Fertilized eggs were exposed to different concentrations of AgNPs in ASW (0.001-1000 µg/L).

A) Percentage of normal D-shaped larvae with respect to controls. The EC<sub>50</sub> reported for AgNP exposure was 23.7 µg/L. B) Percentage of normal D-veliger (white), malformed D-veliger (grey), pre-veligers (black) and trocophora (shaded) in each experimental condition. C1-C3: Representative light microscopy images of control and AgNP-exposed embryos: C1) a normal D-larva; C2) a malformed D-larva showing shell indentations (arrowheads) and protruding mantle (arrow) in samples exposed to 20 µg/L AgNPs; C3) an immature embryo withheld at the trocophora stage in samples exposed to 100 µg/L AgNPs. Scale bars: 20 µm. Data represent the mean ± SD of 3 experiments carried out in 96-multiwell plates (6 replicate wells for each sample).

**Figure 7** - Effects of AgNO<sub>3</sub> on *M. galloprovincialis* larval development in the 48 h embryotoxicity assay. Fertilized eggs were exposed to different concentrations of AgNO<sub>3</sub> (0.1-25 µg/L). A) Percentage of normal D-shaped larvae with respect to controls. The EC<sub>50</sub> reported for AgNO<sub>3</sub> exposure was 1 µg/L. B) Representative light microscopy image of a malformed D-larva exposed to 5 µg/L AgNO<sub>3</sub>. Scale bar: 20 µm. Data, representing the mean ± SD of 3 experiments carried out in 96-multiwell plates (6 replicate wells for each sample).

**A**

Z-average (nm)	Inorganic impurities by ICP-OES ( $\mu\text{g/g}$ )	Surface area by BET ( $\text{m}^2/\text{g}$ )
$61 \pm 20$	Fe: $24 \pm 2$ (LOD: 0.6) Ca: $0.5 \pm 0.1$ (LOD: 0.03)	$3.8 \pm 0.1$

**B**

AgNPs		Z-average (nm)	$\zeta$ -potential (mV)	
Particle suspension	10 mg/L	$138 \pm 20$ (25%)	$-1.5 \pm 3.7$	
		$671 \pm 122$ (75%)		
	ASW	50 mg/L	$130 \pm 22$ (15%) $590 \pm 99$ (85%)	$-1.1 \pm 2.3$
		100 mg/L	$340 \pm 55$ nm (28%) $1600 \pm 340$ nm (72%)	$-1.8 \pm 1.9$
	HS	10 mg/L	$89 \pm 18$ (20%) $473 \pm 57$ (80%)	$-1.5 \pm 3.7$

